From: SHOCK WAVES IN CONDENSED MATTER
Edited by Y.M. Gupta
(Plenum Publishing Corporation, 1986)

LASER INTERFEROMETER MEASUREMENTS OF REFRACTIVE INDEX IN SHOCK-COMPRESSED MATERIALS*

J. L. Wise and L. C. Chhabildas

Thermomechanical and Physical Division
Sandia National Laboratories
Albuquerque, NM

ABSTRACT

Laser interferometer systems provide a means for probing the refractive index of transparent specimens subjected to dynamic compression. Previous interferometer measurements of optical properties under shock loading are reviewed for polymethyl methacrylate, fused silica, sapphire, nitromethane, and an aqueous solution of zinc chloride; various degrees of departure from Gladstone-Dale behavior are noted for these materials. In addition, a detailed summary of recent optical studies of lithium fluoride (LiF) is provided. Interferometer data from plate-impact experiments verify sustained LiF transparency for Hugoniot stresses to at least 160 GPa, and establish the variation of LiF refractive index for shock amplitudes ranging from 1.58 to 115 GPa. The refractive-index data for LiF agree with earlier static and shock-wave data, and exhibit a pronounced deviation from predictions based on the Gladstone-Dale, Lorentz-Lorenz, and Drude relations. A modified form of the Gladstone-Dale relation is presented which correctly models the latest LiF measurements. Potential applications of LiF and other window materials to dynamic high-pressure experimentation are discussed.

INTRODUCTION

Using Doppler-shifted light backscattered from a moving reflector, the laser velocity interferometer (VISAR) developed by Barker and Hollenbach[1] permits time-resolved measurements of the reflector velocity. Application of this technique to impact-response tests on selected target materials often involves a transparent window which is bonded to the rear surface of the target so as to permit velocity measurement at the reflective target/window interface. Analysis of data obtained from such experiments relates the observed interference-fringe count to the reflective-interface velocity in a manner that

*This work performed by Sandia National Laboratories supported by the U. S. Department of Energy under contract #DEAC04-76-DP00789.

must account for a predetermined Doppler-shift correction arising from the strain-induced change in refractive index of the window[1-4]. Conversely, if the dynamic mechanical properties (*i.e.*, Hugoniots) of the impactor, target, and window have been independently determined, then the interferometer data yield a direct measurement of the Doppler-shift correction and refractive index for the shock-compressed window. The present paper begins with an outline of relevant principles governing laser interferometry, then reviews existing interferometer measurements of refractive index for several window materials. Recent results are summarized for lithium fluoride (LiF), and potential window developments and applications are considered.

ANALYSIS OF VISAR RECORDS

Interferometer systems of the VISAR (velocity) or Michelson (displacement) varieties combine two input beams of light to produce a single output beam exhibiting an interference fringe frequency equal to the frequency difference between the input beams. One of the input beams consists of Doppler-shifted light which is reflected from the moving test surface; the other input beam is reference light. For the Michelson interferometer, the reference beam typically has the same frequency as the source laser; however, in some cases[3], the frequency of the reference beam may also be Doppler shifted due to reflection from a surface moving at a known (usually steady) velocity. For the VISAR, the reference beam is a portion of the Doppler-shifted light which has been reflected from the test surface and then separated from the remaining light by means of a beam splitter; this reference beam is then subjected to a time delay τ before recombination with undelayed light. If incident laser light with a wavelength λ_0 is used, then the frequency shift (*i.e.*, Doppler shift) of the backscattered light is $\nu_0 = 2u/\lambda_0$ for reflection from a free surface (*i.e.*, no window) moving at a velocity u. When a reflective surface moving at the same velocity is covered by a window, the frequency shift of the backscattered light is $\nu = \nu_0 + \Delta\nu$, where the correction term, $\Delta\nu$, arises from strain-induced changes in the window refractive index which are a consequence of stress-wave propagation. The expression $(1 + \Delta\nu/\nu_0) = \nu/\nu_0$ represents the ratio of the Doppler shift observed with a window to the frequency shift which would have been observed without a window for a reflector moving at the same velocity. All optical measurements and related analyses discussed in ensuing paragraphs of this paper implicitly apply to experimental times prior to that at which first motion of the window free surface is initiated by stress-wave arrival.

As shown by Barker and Schuler[4], the most general equation expressing the velocity, u, of a reflective interface as a function of the VISAR fringe count, F, is

$$u[t - \frac{1}{2}\tau) = \frac{\lambda_0 F(t)}{2\tau(1 + \delta)(1 + \Delta\nu/\nu_0)}, \qquad (1)$$

where t is time, τ is the user-selected interferometer delay time, λ_0 is the wavelength of the laser light, δ is a correction term for the dependence of etalon refractive index on wavelength of the Doppler-shifted laser light, and $\Delta\nu/\nu_0$ is the frequency correction related to the strain dependence of window refractive index. If fused-silica etalons are used, then $\delta = +0.0239$ for $\lambda_0 = 632.8$ nm (He-Ne laser), and $\delta = +0.0339$ for $\lambda_0 = 514.5$ nm (argon-ion laser).

Characterization of an interferometer window material involves a determination of the strain-dependent behavior of $\Delta\nu/\nu_0$. As discussed by Hardesty[5], the refractive

index, n_H, in the uniaxially strained portion of a window behind a steady, planar shock which propagates into undisturbed material may be derived from $\Delta\nu/\nu_0$ measurements and existing Hugoniot data using the expression

$$n_H = n_0 \frac{U_S}{U_S - u_P} - (1 + \Delta\nu/\nu_0)\frac{u_P}{U_S - u_P}, \tag{2a}$$

where U_S and u_P are, respectively, the shock velocity and Hugoniot particle velocity in the window, and n_0 is the refractive index of unshocked window material. Letting v_H and v_0 represent, respectively, the specific volume of shocked and unshocked window material, the Hugoniot compressive strain is given by $\epsilon_H = (v_0 - v_H)/v_0$, and mass conservation through the shock leads to the following reformulation of equation (2a):

$$n_H = \frac{1}{1 - \epsilon_H}[n_0 - \epsilon_H(1 + \Delta\nu/\nu_0)]. \tag{2b}$$

If a material satisfies the Gladstone-Dale relation, $d\rho/\rho = (n-1)^{-1}dn$ where ρ is the material density, then $\Delta\nu/\nu_0$ must be zero on the basis of equation (2b). Hence, the magnitude of $\Delta\nu/\nu_0$ is a measure of the degree of departure of the refractive index from the Gladstone-Dale model.

PREVIOUS EXPERIMENTAL STUDIES

Solid-state windows consisting of polymethyl methacrylate (PMMA), fused silica, and sapphire have been characterized optically and mechanically in shock-wave studies by Barker and Hollenbach[3]. For the optical studies, a symmetric-impact configuration was employed such that the target specimen and gun-launched impactor were both fabricated from the same window material. In each experiment, a Michelson interferometer yielded a direct measurement of $\Delta\nu$ for a shock-induced particle velocity exactly equal to one-half the measured impact velocity.

For PMMA, the values of $\Delta\nu/\nu_0$ observed by Barker and Hollenbach[3] lie between −0.0022 and −0.0117 for particle velocities ranging from 0.0320 to 0.3173 km/s and corresponding Hugoniot stresses ranging from 0.108 to 1.19 GPa. Subsequent VISAR data obtained by Asay and Hayes[4] show that $\Delta\nu/\nu_0$ for PMMA is zero (to within experimental accuracy) for a shock stress of 5.3 GPa, and work by Lee[7] demonstrates that the $\Delta\nu/\nu_0$ correction is negligible in the 0.5–12.5 GPa range of shock stresses. Later VISAR measurements performed by Chhabildas and Asay[8] with PMMA windows indicate that $\Delta\nu/\nu_0$ is less than 0.02 at 22 GPa. As a consequence of the consistently small magnitude of the $\Delta\nu/\nu_0$ correction for PMMA, the refractive index is closely modeled by the Gladstone-Dale relation for window stresses up to 22 GPa. Above this level, the results of Chhabildas and Asay[8] reveal a loss of transparency (for Hugoniot stresses of 22.5–25 GPa) which has been attributed to an apparent phase transition or molecular dissociation. This loss of transparency precludes any VISAR measurements with PMMA windows subjected to shock stresses in excess of ~22 GPa.

The results reported by Barker and Hollenbach[3] for fused silica show values of $\Delta\nu/\nu_0$ which decrease monotonically from a maximum of 0.0627 at a particle velocity of 0.0713 km/s (stress = 0.905 GPa) to a minimum of 0.0335 at a velocity of 0.571 km/s (stress = 6.53 GPa). These $\Delta\nu/\nu_0$ measurements have been subjected to additional analysis by Setchell[9] to determine the explicit dependence of refractive index

on the density of dynamically compressed specimens. This analysis was motivated by ramp-wave VISAR experiments in which fused silica windows were subjected to time-dependent strain gradients. These gradients created a spatial variation of refractive index within the window which altered the frequency correction needed for proper interpretation of the fringe records. As shown by Setchell, the VISAR equation (1) may be rewritten in terms of a velocity correction, Δu, as

$$u(t - \frac{1}{2}\tau) = \frac{\lambda_0 F(t)}{2\tau(1 + \delta)} - \Delta u \,, \tag{3}$$

where the velocity correction is given by

$$\Delta u = (\Delta\nu/\nu_0)\, u(t - \frac{1}{2}\tau) \,. \tag{4}$$

Setchell noted that the Δu versus Hugoniot particle velocity, u_P, data of Barker and Hollenbach[3] can be accurately represented by a power law:

$$\Delta u = c_1 u_P^{c_2} \,, \tag{5}$$

where the coefficients for a least-squares fit to the fused silica data are $c_1 = 0.02600$ and $c_2 = 0.6680$.

Following Barker[2], Setchell suggested that an appropriate expression linking refractive index to material density may be generated by incorporating a density-dependent correction term $\xi(\rho)$ in the Gladstone-Dale relation; the result is

$$\frac{n - 1}{n_0 - 1} = \frac{\rho}{\rho_0}[1 - \xi(\rho)] \,. \tag{6}$$

Setchell assumed a power-law dependence of $\xi(\rho)$ on density of the form

$$\xi(\rho) = \alpha[(\rho/\rho_0) - 1]^\beta = \alpha[\epsilon/(1 - \epsilon)]^\beta \,, \tag{7}$$

where the parameters α and β are to be determined for a given window material. This determination involves an iterative approach[9] which couples the index/density relation (using trial values of α and β) with conservation and constitutive expressions governing the mechanical response of the material to obtain the density distribution and resultant refractive-index profile through the compressed region of the window. Knowledge of the refractive-index profile then permits calculation of a frequency correction, $\Delta\nu/\nu_0$, and a velocity correction, Δu, corresponding to the trial values of α and β. For a material which supports a single, planar shock, these corrections are obtained directly from equations (2) and (4); however, in the case of fused silica the corrections must be computed on the basis of the combined ramp/shock waveforms produced in the experiments. Different (α, β) trial pairs are selected and used to calculate sets of (u_P, Δu) pairs until a least-squares, power-law fit of the form shown in equation (5) yields coefficients c_1' and c_2' for a calculated (u_P, Δu) set that are equal to the coefficients c_1 and c_2 found earlier by a direct fit to the measured Δu versus u_P data. The values determined in this fashion by Setchell[9] for fused silica are $\alpha = 0.02906$ and $\beta =$

0.6571. Similar to PMMA, a change in response mechanisms places an upper limit on dynamic stresses for which fused silica is a useful window. In particular, Setchell[10] has observed a serious loss in VISAR fringe contrast whenever fused-silica windows are shocked to stresses near or above the elastic limit of approximately 9.8 GPa reported by Wackerle[11] or 8.7 GPa reported more recently by Chhabildas and Grady[12].

Barker and Hollenbach[3] discovered that the optical correction for sapphire samples with axis parallel to the crystallographic Z-axis shows a monotonic decrease from $\Delta\nu/\nu_0 = 0.7771$ for a shock-induced particle velocity of $u_p = 0.0616$ km/s (stress = 2.76 GPa), to $\Delta\nu/\nu_0 = 0.7500$ for $u_p = 0.2875$ km/s (13.15 GPa). Over this range, sapphire exhibits elastic behavior which is slightly nonlinear[3]. As with fused silica, Setchell[9] transformed the frequency corrections to velocity corrections for the sapphire data and applied the power-law fit shown in equation (5) to find the coefficients $c_1 = 0.7307$ and $c_2 = 0.9755$. Using these coefficients and the iterative approach outlined above, Setchell arrived at values of $\alpha = 0.8280$ and $\beta = 0.9606$ to be used in equations (6) and (7) to describe the index/density behavior of sapphire. Barker and Hollenbach[3] detected erratic optical behavior for two shots producing a stress of about 15 GPa in sapphire windows; they concluded that the upper limit of sapphire's usefulness as an elastic window is between 13 and 15 GPa—a stress range which coincides with that predicted for the onset of plastic yielding based on measurements by Graham and Brooks[13] of a Hugoniot elastic limit between 14 and 21 GPa for Z-cut sapphire. However, the possibility of using sapphire windows for stress levels substantially above the elastic regime is supported by VISAR data from a single test performed by Lee[7] which indicates a value of $\Delta\nu/\nu_0 = \sim 0.65$ for a Hugoniot stress of 42.4 GPa in a sapphire window.

The VISAR technique has also been applied to optical measurements on shocked liquids, including studies of nitromethane by Hardesty[8] and an aqueous solution of zinc chloride by Wise[14]. For nitromethane, the experiments by Hardesty[8] over the stress range from 7.5 to 9.5 GPa indicate negative values of $\Delta\nu/\nu_0$ which vary linearly with the density, ρ_H, of the shocked liquid. As determined by Hardesty, a linear, least-squares fit to the data yields $\Delta\nu/\nu_0 = -1.288 + 0.717\rho_H$, and the corresponding refractive-index data are within 2% of the values predicted by the Gladstone-Dale relationship. The results reported by Wise[14] for a 9.1-molar aqueous solution of zinc chloride show positive values of $\Delta\nu/\nu_0$ which vary linearly with the Hugoniot particle velocity, u_p, for shock stresses from 2.18 to 24.1 GPa. A linear, least-squares fit to the data yields $\Delta\nu/\nu_0 = 0.020 + 0.029u_p$. The resultant refractive-index data exhibit increasing departure from the Gladstone-Dale model as the shock amplitude in the zinc-chloride solution is increased; however, the measured refractive index is only 3.1% lower than the Gladstone-Dale value for the highest stress level achieved (24.1 GPa). Subsequent observations on this solution at higher stress levels reveal a loss of solution transparency for shock amplitudes in excess of 25–30 GPa.

STUDIES ON LITHIUM FLUORIDE

As part of an ongoing effort to develop additional window materials for high-pressure interferometry, the optical response of lithium fluoride to shock compression has been investigated in a series of planar (uniaxial strain) impact experiments. These tests have been conducted with several different guns[15] to achieve impact velocities ranging from 0.2 to 5.5 km/s, resulting in LiF window stresses ranging from 1.6 to 115 GPa.

The experimental configuration for these tests is illustrated in Figure 1. An impactor and backing plate are mounted on the forward face of a projectile that is accelerated to a preselected velocity before striking a target which consists of a buffer/window assembly. Prior to target construction, the forward surface of the LiF window is lightly lapped and then vapor plated with an aluminum film ~0.5 μm thick to provide a diffuse reflective surface for the incident laser beam. A thin epoxy bond is used to attach the window to the buffer rear surface, and this assembly is, in turn, potted concentrically within a support ring. Pins mounted around the periphery of the support ring provide measurements of impact velocity and tilt (typically a few milliradians[15]).

The shock impedance (product of shock velocity times initial density) of the backing plate behind the impactor is typically different than that of the impactor itself; consequently, this configuration produces initial Hugoniot states in both the buffer and window which persist for ~1 μs before release or recompression due to arrival of the wave reflected from the backing/impactor interface. If the VISAR fringe count, F, and actual particle velocity, u_p, for the initial Hugoniot state in the window are known, then equation (1) may be solved to determine the frequency correction, $\Delta\nu/\nu_0$. The fringe count is monitored continuously during each experiment and an average value is determined for readings obtained during the initial Hugoniot state; the particle velocity at the reflective interface must be determined independently. For those tests involving a symmetric impact (*i.e.*, LiF buffer and impactor), the particle velocity in the initial shock state is exactly one-half the impact velocity. Otherwise, the particle velocity of the buffer/window interface following arrival of the incident shock may be predicted on the basis of an impedance-matching technique using the measured impact velocity and existing Hugoniot equation-of-state (EOS) data for the impactor, buffer, and window.

All lithium fluoride specimens used in this work are optical-quality single crystals obtained from the Harshaw Chemical Company[16]. The axis of each LiF specimen is oriented parallel to a ⟨100⟩ crystallographic direction. In addition to LiF, other impactor and buffer materials include aluminum (6061), beryllium, copper, sapphire, and tantalum. Relevant Hugoniot EOS parameters used for analysis of the present results are summarized in Table 1 which also includes a description of the initial condition for each material. The parameters c_0 and S listed in Table 1 are coefficients in a linear fit, $U_S = c_0 + Su_p$, to the shock-velocity/particle-velocity Hugoniot for each material.

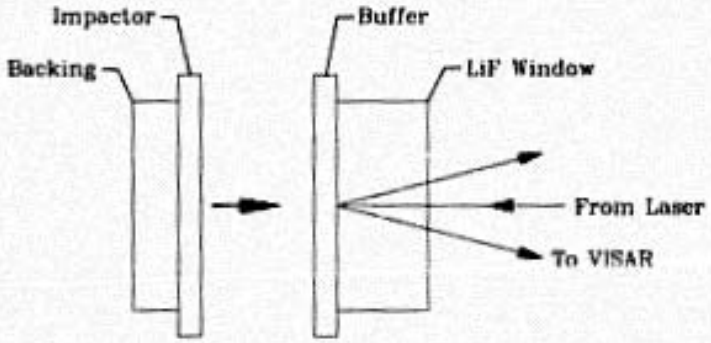

Figure 1: Experimental Configuration for VISAR Studies of Shock-Compressed LiF Windows.

Table 1. Material Specifications and Hugoniot Parameters

Material and Condition	Initial Density (Mg/m^3)	c_0 (km/s)	S	Reference
Al–aluminum (6061-T6)	2.70	5.25	1.35	Herrmann[17]
Al_2O_3–sapphire (single crystal, axis ∥ Z-axis)	3.985	11.19	1.00	Barker, *et al.*[3]
Be–beryllium (polycrystalline)	1.851	7.998	1.124	McQueen, *et al.*[16]
Cu–copper (oxygen-free, high-conductivity)	8.930	3.940	1.489	McQueen, *et al.*[16]
LiF–lithium fluoride (single crystal, axis ∥ ⟨100⟩ direction)	2.640	5.148	1.353	Carter[18]
Ta–tantalum (polycrystalline)	16.654	3.414	1.200	McQueen, *et al.*[16]

Details relating to impact parameters and resultant optical data for individual experiments in this study are displayed in Table 2. The shots are listed in order of increasing window stress and strain. In several cases, two sets of data are reported for a single shot in which two VISARs were used simultaneously; these individual sets are distinguished by appending a "P" (Primary VISAR) or "S" (Secondary VISAR) to the shot number. Except for the first two listings (shots LIF13 and LIF14), all values for window stress and strain have been calculated from the Rankine-Hugoniot relations for a single shock propagating into the window material at a velocity calculated from the linear U_s–u_p relation reported by Carter[18] for stresses ranging from 6.9 to 107.8 GPa in LiF. The highest estimates of window stress, strain, and particle velocity (reported for test LIF12) are based on an extrapolation of Carter's data. At the other extreme, shots LIF13 and LIF14 involve low shock stresses and the effects of the elastic precursor observed in LiF are no longer negligible; hence, the window stress and strain in the initial shock state are obtained by direct integration of the particle-velocity records obtained for these two shots using the respective values of $\Delta\nu/\nu_0$ shown in Table 2.

A review of the information contained in Table 2 reveals that the $\Delta\nu/\nu_0$ data for shock-loaded lithium fluoride show a mean value of 0.281, with a standard deviation of 0.009, for experiments producing window stresses from 10.3 to 115.3 GPa. Over this range, all of the individual $\Delta\nu/\nu_0$ measurements lie within two standard deviations of the mean. Only the two tests (LIF13 and LIF14) involving stresses below 10 GPa indicate $\Delta\nu/\nu_0$ values which are slightly, but measurably, outside the scatter band defined by the remaining data. In general, the main sources of error stem from uncertainties in: (1) projectile-velocity measurement; (2) VISAR fringe count; and, (3) Hugoniot equation-of-state (EOS) parameters. For the low and intermediate projectile velocities which were produced, respectively, by a single-stage gas gun and a propellant (powder) gun, the estimated uncertainty is ±0.2%. The highest projectile velocities (in excess of 2.3 km/s) were attained on a two-stage, light-gas gun and detected with an estimated uncertainty of ±1.0%. Following Barker and Hollenbach[1], estimated uncertainty in the VISAR fringe count is ±0.02. For those shots utilizing a symmetric-impact configuration, uncertainties in EOS data are not a factor. Since the observed scatter in $\Delta\nu/\nu_0$ data for symmetric-impact experiments is comparable to that for impedance-matching

Table 2. Summary of VISAR Experiments on Lithium Fluoride Windows.

Shot Number	Buffer / Impactor Material	Impact Velocity (km/s)	Window Stress (GPa)	Window Strain	Window Particle Velocity (km/s)	Optical Correction $\Delta\nu/\nu_0$	Refractive Index n_{at}
LIF13	LiF / LiF	0.2247	1.576*	0.02136*	0.1124	0.260	1.3968
LIF14	LiF / LiF	0.6021	4.295*	0.05586*	0.3010	0.247	1.4026
BE3P	Be / Al_2O_3	0.8713	10.29	0.1074	0.6471	0.269	1.4089
LIF5P	none[b] / LiF	1.322	10.54	0.1094	0.6610	0.282	1.4076
LIF5S	LiF / LiF	1.322	10.54	0.1094	0.6610	0.268	1.4094
LIF4	LiF / LiF	1.396	11.23	0.1146	0.6980	0.291	1.4072
BE10P	Be / Al_2O_3	0.9462	11.28	0.1150	0.7008	0.268	1.4103
BE10S	Be / Al_2O_3	0.9462	11.28	0.1150	0.7008	0.269	1.4101
LIF3	LiF / LiF	1.616	13.31	0.1295	0.8080	0.277	1.4113
CU17P	Cu / Cu	1.186	13.88	0.1333	0.8373	0.273	1.4125
CU17S	Cu / Cu	1.186	13.88	0.1333	0.8373	0.270	1.4130
AL10	Al / Al	1.755	14.96	0.1403	0.8916	0.281	1.4123
BE1P	Be / Be	1.968	16.70	0.1511	0.9777	0.283	1.4136
BE1S	Be / Be	1.968	16.70	0.1511	0.9777	0.275	1.4151
BE9S	Be / Be	1.984	16.86	0.1520	0.9853	0.274	1.4154
BE11P	Be / Al	1.969	17.15	0.1538	0.9995	0.297	1.4115
LIF2	LiF / LiF	2.021	17.37	0.1550	1.010	0.278	1.4152
BE1P	Be / Be	2.040	17.41	0.1553	1.012	0.294	1.4123
LIF1	LiF / LiF	2.247	19.79	0.1685	1.124	0.271	1.4188
AL20	Al / Al	2.216	19.81	0.1686	1.125	0.288	1.4154
AL5	Al / Al	2.224	19.89	0.1691	1.129	0.279	1.4173
AL1	Al / Al	2.353	20.20	0.1707	1.143	0.283	1.4167
BE13P	Be / Cu	1.962	25.12	0.1947	1.364	0.280	1.4214
BE13S	Be / Cu	1.962	25.12	0.1947	1.364	0.275	1.4226
BE10P	Be / Cu	1.970	25.24	0.1953	1.367	0.286	1.4204
BE10S	Be / Cu	1.970	25.24	0.1953	1.367	0.286	1.4204
BE15P	Be / Cu	1.987	25.51	0.1965	1.378	0.285	1.4205
BE6P	Be / Cu	2.000	25.71	0.1974	1.387	0.299	1.4172
BE6S	Be / Cu	2.000	25.71	0.1974	1.387	0.289	1.4197
CU19P	Cu /Cu	2.020	26.47	0.2007	1.412	0.286	1.4210
LIF9	none[b] / Ta	3.473	60.90	0.3030	2.644	0.286	1.4408
LIF11P	LiF / Ta	5.028	102.3	0.3682	3.778	0.277	1.4620
LIF11S	LiF / Ta	5.028	102.3	0.3682	3.778	0.272	1.4649
LIF12P	LiF / Ta	5.459	115.3	0.3829	4.090	0.288	1.4596
LIF12S	LiF / Ta	5.459	115.3	0.3829	4.090	0.292	1.4571

*Obtained by direct integration of particle-velocity record.
[b]VISAR measurement made at impact surface.

experiments, no attempt has been made to quantify EOS uncertainties affecting interpretation of results from the impedance-matching experiments.

Using equation (4), the $\Delta\nu/\nu_0$ data have been converted to velocity corrections, Δu, which are plotted as a function of the Hugoniot particle velocity, u_p, in Figure 2. Estimated error bars are displayed for the impedance-matching experiments which used tantalum impactors to achieve the highest shock stresses; error bars for symmetric-impact tests are contained by the plotted points. A least-squares, power-law fit of the form shown in equation (5) has been performed for all 35 Δu–u_p pairs, and the resulting

coefficients are $c_1 = 0.2784$ and $c_2 = 1.031$ for lithium fluoride. This power-law fit is also plotted in Figure 2.

As discussed earlier, each $\Delta\nu/\nu_0$ datum provides a measurement of the refractive index. For the present study, the refractive index is obtained directly from equation (2) which, strictly speaking, applies only to the case of a single shock propagating into undisturbed material. In lithium fluoride, the refractive index determined in this manner is exact (to within experimental accuracy) for shock stresses in excess of ~18 GPa since the precursor is overdriven. At lower shock stresses, the observed frequency correction, $\Delta\nu/\nu_0$, is a consequence of changes in refractive index through both the precursor and the shock. To investigate the effect of elastic-plastic window response on the relationship between the refractive index and the Doppler-frequency correction, $\Delta\nu/\nu_0$, an analysis has been performed for a two-wave loading profile consisting of a steady elastic precursor and a trailing steady shock which propagate at velocities relative to undisturbed window material of c_l and U_S, respectively. Under these conditions the refractive index, n_H, of the shock-processed material is given by

$$n_H = n_0 \frac{c_l}{U_S - u_P} - n_1 \frac{c_l - U_S}{U_S - u_P} - (1 + \Delta\nu/\nu_0) \frac{u_P}{U_S - u_P} \quad (8)$$

where n_1 is the refractive index of material between the precursor and shock. As expected, equation (8) reduces to equation (2a) when $n_1 = n_0$ (no precursor), or when $c_l = U_S$ (precursor just overdriven). Thus, a determination of the refractive index in the final Hugoniot state requires an independent means (experimental or analytical) for specifying the refractive index, n_1, in material which has been processed by the precursor only. If an assumption is made that the change in refractive index through the precursor can be estimated using the Gladstone-Dale relation, existing data for the precursor velocity and amplitude in LiF (e.g., see Asay, et al.[26]) yield an

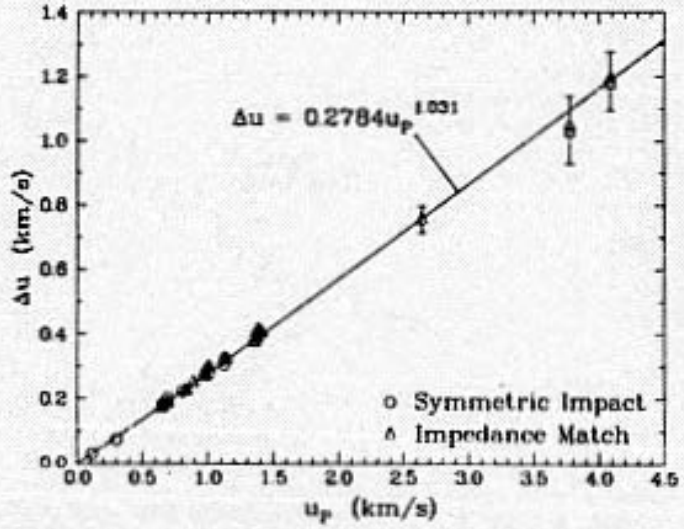

Figure 2: Velocity Correction, Δu, for VISAR Data Influenced by Refractive-Index Effects in Lithium Fluoride.

estimate for n_1 which is ~0.10% larger than n_0, and equation (8) may subsequently be solved to determine n_H for those experiments producing a shock stress below 18 GPa in the window. Values of n_H calculated in this fashion are within 0.00–0.05% of the values calculated using equation (2) where the effects of the precursor were ignored. This agreement is well within the estimated experimental uncertainty, and the use of equation (2) is consequently justified. The resultant refractive-index data are listed in Table 2 and are plotted as a function of compressive strain in Figure 3.

For comparison to the present data, predicted variations of refractive index with strain based on the Gladstone-Dale, Lorentz-Lorenz, and Drude models are also plotted in Figure 3. The integrated form of the Gladstone-Dale relation is

$$\frac{1}{\rho}(n-1) = constant\ . \tag{9}$$

In the case of the Lorentz-Lorenz model, the index/density relation is given by

$$\frac{1}{\rho}\frac{(n^2-1)}{(n^2+2)} = constant\ ; \tag{10}$$

whereas the Drude expression is

$$\frac{1}{\rho}(n^2-1) = constant\ . \tag{11}$$

An examination of Figure 3 quickly reveals that all of these models fail to provide a fit to the data for lithium fluoride; hence, a semi-empirical index/density relationship of the type shown in equations (6) and (7) has been attempted. However, the correction term $\xi(\rho)$ given by equation (7) results in an index/strain relation which, contrary to the

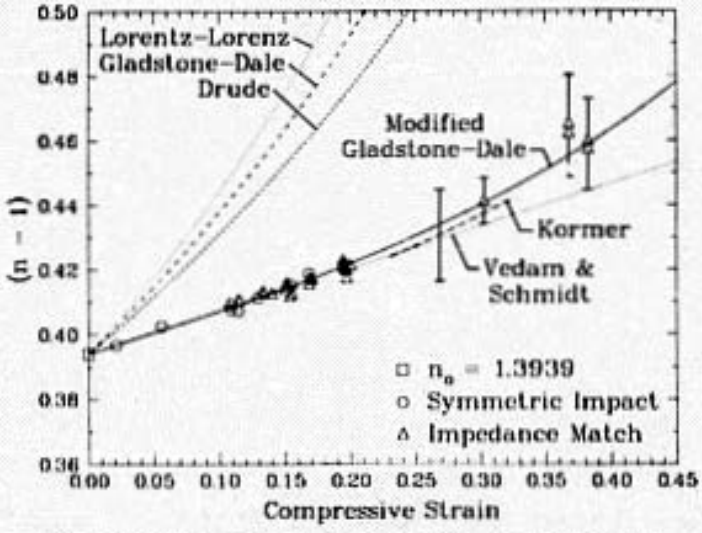

Figure 3: Strain Dependence of LiF Refractive Index.

present data, is convex upward and predicts decreasing values of refractive index for strains greater than ~0.38. An excellent fit to the present data has been achieved by adopting an alternate functional form for $\xi(\rho)$ given by

$$\xi(\rho) = \gamma|1 - (\rho_0/\rho)|^{\kappa} = \gamma\epsilon^{\kappa} , \qquad (12)$$

where γ and κ are constants to be determined using the same iterative approach outlined earlier which assures that a power-law fit to the set of $(u_P, \Delta u)$ values calculated on the basis of the index/density relations (6) and (12) yields the same coefficients obtained for a power-law fit to the actual $(u_P, \Delta u)$ measurements. For the present data, the appropriate coefficients for LiF are $\gamma = 0.7630$ and $\kappa = 1.040$. Using the dispersion formula and constants reported by Herzberger and Salzberg[21], the initial refractive index, n_0, of LiF is 1.3939 for $\lambda_0 = 514.5$ nm. With this value of n_0 and the experimentally determined values of γ and κ, equations (6) and (12) have been used to calculate the locus of refractive index versus compressive strain (labelled "Modified Gladstone-Dale") which is plotted along with the individual data points in Figure 3.

Previous refractive-index data for shock-loaded LiF have been reported by Kormer[22] over a more limited range of strain ($\epsilon_H = 0.231$–0.324). For this work, an explosive driver system in direct contact with a flat surface of the test specimen generated a planar shock (parallel to the driver surface) which propagated into the transparent material. A collimated beam of light from an explosive source was transmitted into the unshocked portion of the specimen so as to be obliquely incident upon the moving shock front. This incident light was partially reflected by the shock itself; the remaining light entered the compressed portion of the specimen and was obliquely reflected by the rear surface which was in contact with the driver system. A high-speed streak camera recorded the relative locations of these two obliquely reflected beams after they emerged from the test assembly, and the refractive index under shock loading was subsequently inferred using geometric optics and the independently determined compressive strain in the transparent specimen.

For several alkali halides, including LiF, Kormer[22] found that the relationship between the refractive index and density may be written as

$$n_H(\sigma_H) = n_0 + \frac{dn_H}{d\sigma_H}(\sigma_H - 1) , \qquad (13)$$

where $\sigma_H = \rho_H/\rho_0$ is the compression and $dn_H/d\sigma_H$ is a constant with a different characteristic value for each crystal. Over the range of his reported data ($\sigma_H = 1.30$–1.48), Kormer reports a value of $dn_H/d\sigma_H = 0.1$ for LiF. The initial index, n_0, listed by Kormer for LiF is 1.392 for the broadband light from his explosive source, whereas $n_0 = 1.3939$ for incident light from an argon-ion laser ($\lambda_0 = 514.5$ nm). Measurements made under broadband lighting with a Bausch & Lomb Abbe-3L refractometer confirm that $n_0 = 1.3925$ for representative LiF samples used in the present studies. However, for comparison to the VISAR results, equation (13) has been used with $n_0 = 1.3939$ to construct a locus for the Kormer data which is shown in Figure 3. The single error bar centered on this line corresponds to Kormer's estimated accuracy of 1–2% for n/n_0.

The refractive index of LiF under hydrostatic pressure has been investigated by Vedam and Schmidt[23]. Results from this study show that the index increases linearly

with pressure to at least the maximum observed loading of 0.7 GPa, corresponding to a volume (compressive) strain, $\epsilon = (v_0 - v)/v_0$, of 0.01. A linear fit to the index/strain data yields $n - n_0 = 0.132\epsilon$ for $0 \leq \epsilon \leq 0.01$. Although the maximum strain achieved in the hydrostatic pressure tests is substantially below the range covered by the shock-compression studies ($\epsilon_H = 0.02$–0.38), an extrapolation of the linear fit to the Vedam and Schmidt data (using $n_0 = 1.3939$) shows very good agreement with shock-wave data for strains up to ~0.20–0.25 (see Figure 3). Above this level, the shock-wave measurements indicate an increasing departure from the linear index/strain relation.

The present measurements extend the available optical data for LiF to substantially higher and lower dynamic strain states than previously investigated. Sustained transparency of LiF has been confirmed to at least the highest shock amplitude (115.3 GPa) achieved in these studies, and a more recent VISAR experiment by Grady[34] verifies LiF transparency for an estimated Hugoniot stress of 160 ± 10 GPa. Comparison of the two existing sets of refractive-index data on shock-compressed LiF over the shared range of Hugoniot strain demonstrates an excellent agreement between the present results (based on interference techniques) and Kormer's results[32] (determined by geometric optics).

DISCUSSION

The laser interferometer measurements of refractive index described in preceding sections of this paper stem from efforts to develop appropriate window materials to support interferometric monitoring of dynamic response for a wide variety of test specimens. Solid-state materials sufficiently characterized for use as interferometer windows now include lithium fluoride, PMMA, sapphire, and fused silica; optically calibrated liquid-state materials include a 9.1-molar aqueous solution of zinc chloride and nitromethane (a liquid explosive). Transparency under anticipated levels of shock loading is the obvious factor governing selection of a window material for a particular application; from this standpoint, lithium fluoride is presently the most versatile candidate by virtue of its sustained transparency for shock stresses to at least 160 GPa.

A requirement typically placed on a window is that its shock impedance closely match the impedance of the target material which it contacts, thereby minimizing release or recompression of the target following wave interaction with the target/window interface. The intermediate shock impedance of lithium fluoride is a very close match to such technically important materials as aluminum and beryllium. High-impedance materials, such as copper, steel, and uranium, are best paired with sapphire windows for an impedance match, whereas low-impedance materials, such as polymeric compounds and condensed explosives, are best matched by fused silica, PMMA, and liquid windows. Liquid solutions offer the unique possibility of tailoring the shock impedance over a wide range by variation of the solute concentration. By directly wetting the surface of the target material, liquid windows may also prove advantageous for applications such as shock rise-time measurements where the epoxy bond typically found between the target and a solid-state window can create an impedance mismatch which substantially complicates data analysis.

The continuing development of new dynamic loading and measurement techniques will necessarily involve parallel efforts to optically characterize suitable window materials. New loading capabilities at ultra-high pressures are anticipated for rail-gun

and laser facilities where optical measurements will undoubtedly benefit from window for shock stresses well in excess of 100 GPa. The increasing use of experimental geometries which employ oblique impact[25] or anisotropic crystals[26] to generate coupled pressure-shear response in target materials will benefit from the development of high-shear-strength windows and bonding methods such as that reported by Chhabildas[26]. Windows have already been employed by Barker[27] in experiments involving the generation and observation of quasi-isentropic compressional waves. Barker[28] has suggested that the smaller temperature rise and strain rate associated with a quasi-isentropic wave as compared to a shock wave with the same peak pressure may lead to window transparency limits at stresses much higher than the limiting values under shock compression. Other window applications include, for example, the infrared radiometry and hot-spot photography reported by Von Holle[29] for studies of inert and reactive (explosive) materials experiencing shock compression. The rapidly expanding fiber-optic technology may also result in new diagnostic probes which require (or permit) optical characterization of additional window materials and geometries and/or the fiber itself under dynamic loading.

REFERENCES

1. L. M. Barker and R. E. Hollenbach, Laser Interferometer for Measuring High Velocities of Any Reflecting Surface, J. Appl. Phys. 43:4669 (1972).
2. L. M. Barker, Fine Structure of Compressive and Release Wave Shapes in Aluminum Measured by the Velocity Interferometer Technique, in: "Behaviour of Dense Media under High Dynamic Pressures," Gordon and Breach, New York (1968).
3. L. M. Barker and R. E. Hollenbach, Shock-Wave Studies of PMMA, Fused Silica, and Sapphire, J. Appl. Phys. 41:4208 (1970).
4. L. M. Barker and K. W. Schuler, Correction to the Velocity-per-Fring Relationship for the VISAR Interferometer, J. Appl. Phys. 45:3692 (1974).
5. D. R. Hardesty, On the Index of Refraction of Shock-Compressed Liquid Nitromethane, J. Appl. Phys. 47:1994 (1976).
6. J. R. Asay and D. B. Hayes, Shock-Compression and Release Behavior Near Melt States in Aluminum, J. Appl. Phys. 46:4789 (1975).
7. L. M. Lee, Shock-Induced Index-of-Refraction Variations in PMMA, Sapphire, and Lithium Fluoride, Ktech Corp. Report TR-76-04 (1976).
8. Lalit C. Chhabildas and James R. Asay, Rise-time Measurements of Shock Transitions in Aluminum, Copper, and Steel, J. Appl. Phys. 50:2749 (1979).
9. Robert E. Setchell, Index of Refraction of Shock-Compressed Fused Silica and Sapphire, J. Appl. Phys. 50:8186 (1979).
10. Robert E. Setchell, Ramp-Wave Initiation of Granular Explosives, Combust. Flame 43:255 (1981).
11. Jerry Wackerle, Shock-Wave Compression of Quartz, J. Appl. Phys. 33:922 (1962).
12. L. C. Chhabildas and D. E. Grady, Shock Loading Behaviour of Fused Quartz, in: "Shock Waves in Condensed Matter-1983," J. R. Asay, R. A. Graham, and G. K. Straub, ed., North-Holland, Amsterdam (1984).
13. R. A. Graham and W. P. Brooks, Shock-Wave Compression of Sapphire from 15 to 420 kbar. The Effects of Large Anisotropic Compressions, J. Phys. Chem. Solids 32:2311 (1971).

14. J. L. Wise, Refractive Index and Equation of State of a Shock-Compressed Aqueous Solution of Zinc Chloride, in: "Shock Waves in Condensed Matter 1983," J. R. Asay, R. A. Graham, and G. K. Straub, ed., North-Holland, Amsterdam (1984).
15. Lalit C. Chhabildas, The Sandia Shock Thermodynamics Applied Research Facility, in: "Shock Waves in Condensed Matter–1981," W. J. Nellis, L. Seaman, and R. A. Graham, ed., American Institute of Physics, New York (1982).
16. The Harshaw Chemical Company, Crystal & Electronic Products, Solon, Ohio.
17. W. Herrmann, Development of a High Strain Rate Constitutive Equation for 6061-T6 Aluminum, Sandia Report SLA-73-0897 (1974).
18. R. G. McQueen, S. P. Marsh, J. W. Taylor, J. N. Fritz, and W. J. Carter, The Equation of State of Solids from Shock Wave Studies, in: "High-Velocity Impact Phenomena," Ray Kinslow, ed., Academic Press, New York (1970).
19. W. J. Carter, Hugoniot Equation of State of Some Alkali Halides, High Temp.-High Press. 5:313 (1973).
20. J. R. Asay, G. R. Fowles, G. E. Duvall, M. H. Miles, and R. F. Tinder, Effects of Point Defects on Elastic Precursor Decay in LiF, J. Appl. Phys. 43:2132 (1972).
21. Max Herzberger and Calvin D. Salzberg, Refractive Indices of Infrared Optical Materials and Color Correction of Infrared Lenses, J. Opt. Soc. Am. 52:420 (1962).
22. S. B. Kormer, Optical Study of the Characteristics of Shock-Compressed Condensed Dielectrics, Sov. Phys. Usp. 11:229 (1968).
23. K. Vedam and E. D. D. Schmidt, Effect of Hydrostatic Pressure on the Refractive Index of LiF, Solid State Commun. 3:373 (1965).
24. D. E. Grady, Sandia National Laboratories, private communication.
25. A. S. Abou-Sayed, R. J. Clifton, and L. Hermann, The Oblique-Plate Impact Experiment, Exp. Mech. 16:127 (1976).
26. Lalit C. Chhabildas, Dynamic Transverse Particle Velocity Measurements using Interferometric Techniques, in: "High Speed Photography, Videography, and Photonics," Dennis L. Paisley, ed., Proc. SPIE 427 (1983).
27. L. M. Barker, High-Pressure Quasi-Isentropic Impact Experiments, in: "Shock Waves in Condensed Matter–1983," J. R. Asay, R. A. Graham, and G. K. Straub, ed., North-Holland, Amsterdam (1984).
28. L. M. Barker, Sandia National Laboratories, private communication.
29. William G. Von Holle, Shock Wave Diagnostics by Time-Resolved Infrared Radiometry and Non-Linear Raman Spectroscopy, in: "Shock Waves in Condensed Matter–1983," J. R. Asay, R. A. Graham, and G. K. Straub, ed., North-Holland, Amsterdam (1984).